



Cite this: *Org. Biomol. Chem.*, 2022, **20**, 7056

Received 30th June 2022,
Accepted 3rd August 2022

DOI: 10.1039/d2ob01176j

rsc.li/obc

Amidosquaramides – a new anion binding motif with pH sensitive anion transport properties†

Luke A. Marchetti,^a Tobias Krämer  ^a and Robert B. P. Elmes  ^{a,b}

Stimuli responsive anion transport is becoming an important aspect of supramolecular anion recognition chemistry. Herein, we report the synthesis of a family of anion receptors that incorporate a new anion binding motif, amidosquaramides. We show using experimental and computational methods that these receptors have pK_a values close to physiological pH but also display intramolecular H-bonding interactions that affect anion recognition. Moreover, moderate activity in a $\text{Cl}^-/\text{NO}_3^-$ exchange assay is observed at physiological pH that can be effectively 'switched on' when repeated under acidic conditions. The reported findings provide synthetic methods that can be used for the construction of more complex squaramide based anion receptors and also provide insight into the importance of conformational analysis when considering receptor design.

Introduction

Squaramides, a family of conformationally rigid cyclobutene ring derivatives, are rapidly gaining research interest across diverse areas of the chemical and biological sciences.¹ Composed of two carbonyl hydrogen-bond acceptors in close proximity to two NH hydrogen-bond donors, this small molecular scaffold benefits from unique physical and chemical properties that render it extremely useful in the design of anion receptors^{2,3} and transporters.^{4,5} This has led to an explosion of research in the area of supramolecular medicinal chemistry where efficient anion transporters have been explored as treatment options for a variety of disease states including anti-cancer agents,^{6,7} CF treatments,⁸ and anti-microbial agents.⁹ The use of squaramides in this regard has been accelerated by their synthetic versatility, strong H-bond donating ability, planar structure and an increase in aromaticity upon guest binding¹⁰ – all properties that make squaramides practical for use in a wide variety of medicinal chemistry applications more broadly. However, if the full potential of squaramides are to be realised, further strategies are required to increase their structural diversity while simultaneously increasing their anion binding affinity.

One approach that has not been considered in the context of squaramide synthesis is a reversal of reactivity. The large majority of the synthetic literature uses a method developed by

Cohen *et al.*¹¹ where diethylsquarate is employed as an electrophile in a substitution reaction with a primary amine to form an *N*-aryl or alkyl linkage. A lesser explored route is the exploitation of a squaramide as a nucleophile in a condensation reaction to form an *N*-amide linkage. While the amine's nucleophilicity is considerably reduced by proximity to two carbonyl groups within the cyclobutene ring, this option should give access to a broader subset of possible receptors. Davis *et al.* reported such a route where they synthesised *N*-carbamoyl squaramides and described their self-assembly behaviour, however, anion binding characteristics were not reported.¹²

Several methods have been used to increase the anion binding affinity of squaramides. Incorporation of an electron withdrawing aromatic substituent can improve H-bond donor ability,¹³ however, limitations arise where acidity of NHs can be pursued to a level that favours deprotonation by basic anions.^{14,15} Similarly, inclusion of several squaramide binding sites within a single molecule can give rise to high affinity supramolecular receptors but this can also lead to issues of solubility.^{16,17}

We envisaged that the *N*-amido linkage previously reported by Davis *et al.* could be exploited as an anion binding moiety and their synthetic approach could be expanded to produce a more diverse range of anion receptors. Herein, we describe the synthesis of a family of disubstituted squaramides using this approach that allows incorporation of both an *N*-aryl linkage and an *N*-amide linkage in the same molecule; so called 'amidosquaramides' (Fig. 1). Varying the substituents of these phenyl moieties, allowed us to investigate the effect on the amidosquaramides anion binding affinity in comparison to their parent squaramide. We envisaged that the *N*-amide

^aDepartment of Chemistry, National University of Ireland Maynooth, Maynooth, Ireland. E-mail: robert.elmes@mu.ie

^bSynthesis and Solid State Pharmaceutical Centre (SSPC), Ireland

† Electronic supplementary information (ESI) available. See DOI: <https://doi.org/10.1039/d2ob01176j>



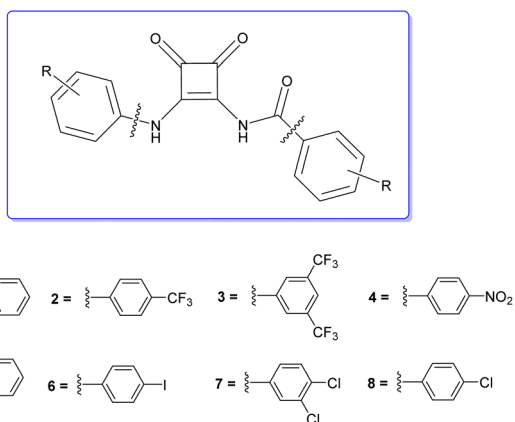


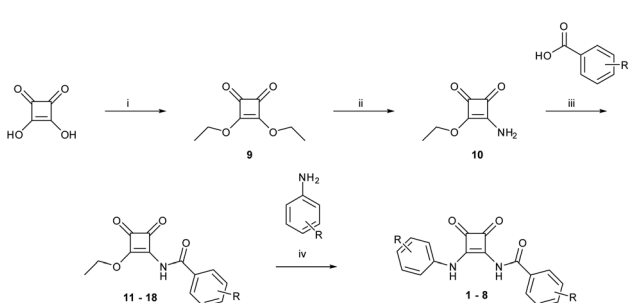
Fig. 1 Structure of amidosquaramides.

linkage would increase the acidity of the squaramide NH, consequently decreasing its pK_a , and increasing its anion binding affinity. We have conducted a detailed spectroscopic and computational analysis of their structure, anion recognition ability, and a preliminary analysis of their anionophoric activity.

Results and discussion

Synthesis

Amidosquaramides were accessed through a linear synthetic approach (Scheme 1). Initially, diethyl squareate was obtained using methods adapted by Moore *et al.*,¹⁸ which was then converted to amino-squarate using methods previously reported by Davis *et al.*¹² The *N*-amide linkage was then formed by coupling the amino-squarate to the relevant benzoic acid derivative using EDCI-HCl. The yield of the coupling reactions varied greatly (25–83%), depending on the strength of the electron-withdrawing groups of the benzoic acid substituents, where the stronger electron-withdrawing groups resulted in lower yields. With the example of 11, the successful formation of the *N*-amido linkage was indicated in the ^1H NMR where the amido-NH signal appeared at 9.88 ppm (see ESI†).



Scheme 1 Synthetic pathway to amido-squaramides. Reagents and conditions: (i) triethyl orthoformate, EtOH, 80 °C, 72 h, 91%; (ii) 20% ammonium in ethanol, EtOH, rt, 18 h, 70%; (iii) EDCI-HCl, DMAP, MeCN/DMF (anhydrous), N_2 , rt –80 °C, 18 h, 10–83%; (iv) $\text{Zn}(\text{OTf})_2$, MeCN/DMF, 80 °C, 3–18 h, 10–71%.

The final step of the synthetic pathway was a substitution reaction between the amidosquare intermediate and the relevant aniline in the presence of zinc trifluoromethanesulfonate, acting as a Lewis-acid catalyst, to yield the target amidosquaramides. The yields of this final step again depended on the electron-withdrawing ability of the aryl substituents, ranging from 10–71%. Synthesis of the target amidosquaramides was evidenced by the presence of a new resonance signal appearing at 11.95 ppm, in the example of 1, attributed to the phenyl-NH proton and the slight downfield shift of the *N*-amide proton signal to 9.98 ppm (see ESI†). The successful synthesis of compounds 1–8 was confirmed in all cases by ^1H and ^{13}C NMR, infrared spectroscopy (IR) and high-resolution mass spectrometry (HRMS) (see ESI† for further details).

pK_a determination

pK_a is a key parameter when considering the anion recognition properties of charge neutral anion receptors. Thus, to examine the effect the carbonyl has on the pK_a of the amido-NH, pH-spectrophotometric titrations were performed to obtain experimental pK_a values, using a method described by Schmidchen *et al.*¹⁹ These titrations were performed in a mixture of DMSO–water (9/1 v/v; in the presence of 0.1 M TBAPF₆ at a receptor concentration of 10 μM).

During the spectrophotometric titrations, deprotonation events were observed by hypo- and hyperchromism of absorbance bands at various wavelengths. This can be seen in the example of 6 (Fig. 2), where there hypochromism occurs at 284 and 320 nm and hyperchromism at 347 and 407 nm, signalling deprotonation events. The inset of Fig. 2 details the changes of absorbance as a function of pH. A four-parameter sigmoid curve was fitted through these data points using Sigma Plot (Systat Software Inc., Chicago, IL, USA) with the point of inflection corresponding to the pK_a , the results of which are summarised in Table 1. We expected to observe two deprotonation events, one for the amide-NH and the second being the NH of the phenyl substituent, however, only one deprotonation could be observed for all receptors. This sig-

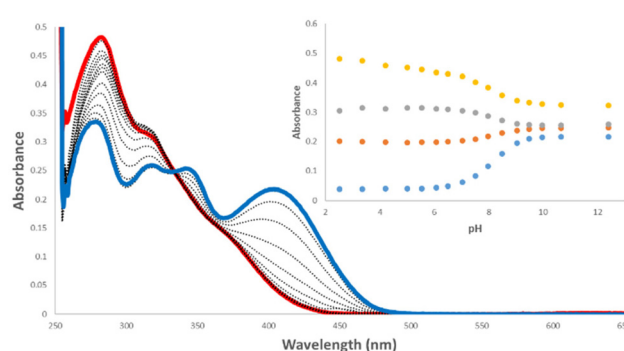


Fig. 2 Absorption spectra taken over the course of a pH-spectrophotometric titration of 6 (10 μM) in an DMSO–water mixture (9/1 v/v; in presence of 0.1 M TBAPF₆) pH 2.52 (blue), pH 12.40 (red). Inset: Comparison plots of absorbance at 284 nm (yellow), 320 nm (grey), 347 nm (orange), and 407 nm (blue) vs. pH.

Table 1 Summary of experimentally obtained pK_a values for *N*-phenyl NH and calculated values for both *N*-phenyl and *N*-amide NH

Receptor	<i>N</i> -Amide pK_a (exp.)	<i>N</i> -Amide pK_a (calc.)	<i>N</i> -Phenyl pK_a (calc.)
1	8.8	8.7	12.7
2	7.3	7.9	11.6
3	6.3	6.6	10.3
4	7.5	7.5	10.4
5	8.8	8.9	12.4
6	8.1	9.8	11.4
7	7.1	7.1	9.3
8	8.2	7.8	11.0

fied that the pK_a of only one NH was determined during these experiments.

We postulated that the pK_a of the *N*-amide NH would be lower than that of the *N*-phenyl pK_a due to the electron-withdrawing effect of the carbonyl. Thus, examining the results of the pH-spectrophotometric titrations, we expected that we had determined the pK_a values of the amide-NH as they displayed lower pK_a values than those of analogous disubstituted *N*-phenyl squaramides.²⁰ This was the first piece of evidence suggesting that inclusion of a carbonyl on the squaramide NH increases its acidity.

To confirm the validity of our experimental pK_a values and to establish an approximate pK_a for both the *N*-phenyl and *N*-amide NH, quantum chemical calculations were undertaken (full details are given in the ESI†). All receptors and their conjugated bases were subjected to unconstrained geometry optimisations at the M06-2X/6-31+G(d) level of theory, following initial exploration of their conformational space with the conformer-rotamer ensemble sampling tool (crest).²¹ Thermal and entropic corrections were evaluated within the rigid rotor harmonic oscillator approximation. High-level single point calculations using the DLPNO-CCSD(T) method were performed on the above geometries. From these calculations, the energy-minimised structure of receptor 1 and its derivatives showed that the carbonyl of the amide-linkage participates in an intramolecular hydrogen bond to the NH of the *N*-phenyl NH (Fig. 3(a)).

Reinforcing the finding that the amidosquaramide prefers to maintain a planar conformation stabilised by H-bonding, molecular dynamics simulations of 1 furnish the free energy surface of the system's conformational space as illustrated in the heat map shown in Fig. 3(a). The conformational space is defined by the two torsional angles C-C-N-C(Phenyl) (θ) and C-C-N-C(=O) (φ), *i.e.* rotations around the bonds attached to the double bond of the cyclobut-3-ene ring of the squaramide. The heat map shows two distinct minima (blue) of the amidosquaramide conformations, one where the amidosquaramide adopts an *anti/syn* conformation as it participates in intramolecular H-bonding and one where the amidosquaramide adopts an *anti/anti* conformation.

pK_a values of all receptors were obtained using a direct method *via* the thermodynamic cycle depicted in Scheme 2. Solvation free energies in DMSO were obtained using the SMD

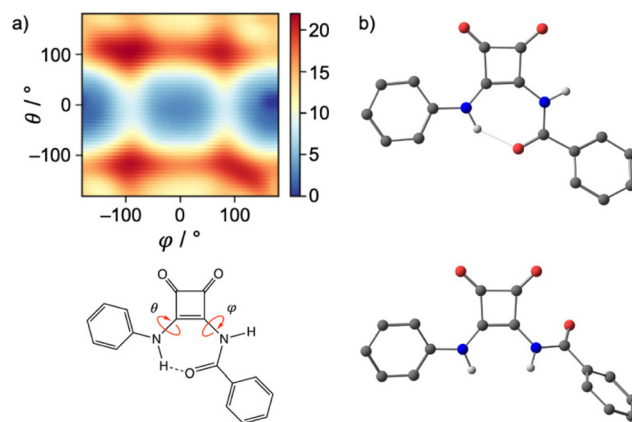
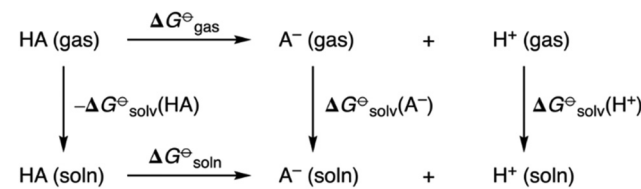


Fig. 3 (a) Gibbs Free Energy heat map (in kcal mol⁻¹) of conformational space of **1** illustrating two minima (blue). (b) The two lowest energy conformations of **1**, *anti/syn* (top), *anti/anti* (bottom). Hydrogens bound to carbon have been omitted.



Scheme 2 Thermodynamic cycle for quantum chemical prediction of pK_a values of amidosquaramide receptors.

implicit solvent model and utilising solvent-reoptimized geometries. A proton solvation free energy of -273.30 kcal mol⁻¹ in DMSO was used.²²

The results obtained showed excellent agreement between the experimentally and computationally derived pK_a values (Table 1). The calculated values of the *N*-phenyl NH also show alignment with previous reports in the literature from Ni *et al.*²³ Moreover, the observed values correlate with the Hammett constants of the substituents *i.e.* the pK_a of the receptor decreases as the Hammett constant increases.²⁴ For example, receptor 3 bearing two (trifluoromethyl) moieties displayed the lowest pK_a while the unsubstituted receptor 1 displayed the highest pK_a . The calculations also confirmed that the *N*-amide linkage decreased the pK_a of the amidosquaramide receptors. Although the conditions should have allowed it, we did not observe a 2nd deprotonation event spectroscopically. This suggests that either the 2nd deprotonation is not observed by absorption spectroscopy or the computational values are not accurate. We have previously observed a 2nd deprotonation spectroscopically in a squaramide-anthracene conjugate whereby titration with TBAOH, resulted in stark spectroscopic changes on going from the mono-deprotonated species to the doubly deprotonated derivative.²⁵ While the 2nd pK_a for this compound was not calculated it suggests that strongly basic conditions are required to effect a 2nd deprotonation. Moreover, it is known that squaramides are not stable



at highly basic pH,²⁶ and this may explain why we were not able to observe a 2nd clear equivalence point.

Given the observed propensity of amidosquaramides to possibly form an intramolecular H-bond, we expected that this may impact on the anion binding ability of this receptor. Indeed, we envisaged that it may cause an additional thermodynamic barrier to anion recognition where the intramolecular interaction would first need to be overcome and a conformational change induced before anion recognition could proceed.

Anion binding studies

Receptors **1–3** were selected to undergo ¹H NMR spectroscopic anion screening to assess their interaction in DMSO-*d*₆ (0.5% H₂O) with a range of TBA salts of halides and oxoanions (F, Cl, Br, I, NO₃, AcO, H₂PO₄²⁻, SO₄²⁻).

When treated with basic anions (F⁻, AcO⁻ and H₂PO₄²⁻) all receptors underwent deprotonation. This was observed in the ¹H NMR spectra with the disappearance of both NH peaks and in some cases, the coalescence of aromatic peaks (see ESI†). In the case of TBAF, the formation of HF₂⁻ can be seen by the characteristic peak at 16.15 ppm (see ESI†). Minimal observable changes in the ¹H NMR spectra were observed when receptors were treated with 10 molar equivalents of Br⁻, I⁻ or NO₃⁻ indicating that little interaction was taking place. SO₄²⁻ exhibited quite different behaviour from other anions whereby a broad NH peak at ~9.5 ppm was observed that was absent with the other anions. Moreover, the aromatic signals were also significantly perturbed suggesting that more complex behaviour is occurring with this anion. When treated with 10 molar equivalents of Cl⁻, a downfield shift of the amido-NH was observed (Δ ppm \approx 1) indicating stronger hydrogen bond formation between this anion and the receptors.

Based on the results of the anion screen, more detailed ¹H spectroscopic titrations were performed in DMSO-*d*₆ (0.5% H₂O) at 298 K, to determine the binding constants for Cl⁻. All receptors displayed similar behaviour when treated with TBACl. Sequential additions of Cl⁻ resulted in the NH peak corresponding to the amido-NH (blue) undergoing a downfield shift, while the NH peak corresponding to the *N*-phenyl (green) displayed a barely discernible shift, as seen with **3** as an example (Fig. 4). Slight shifts in aromatic resonances could also be observed, possibly indicating weak C–H···anion interactions.

As the results of the geometry optimisation showed the amidosquaramides contain an intramolecular H-bond between the *N*-phenyl NH and the amide's oxygen atom, it is unsurprising that there was only a slight shift observed for the corresponding signal when treated with TBACl. We postulate that the stability afforded by the intramolecular H-bond results in the amidosquaramide being unwilling to break this intramolecular interaction, resulting in only one NH being available to bind to anionic guests.

Binding constants were determined by plotting the changes in chemical shift of the NH peaks against anion concentration and the resulting plots were analysed using the open access

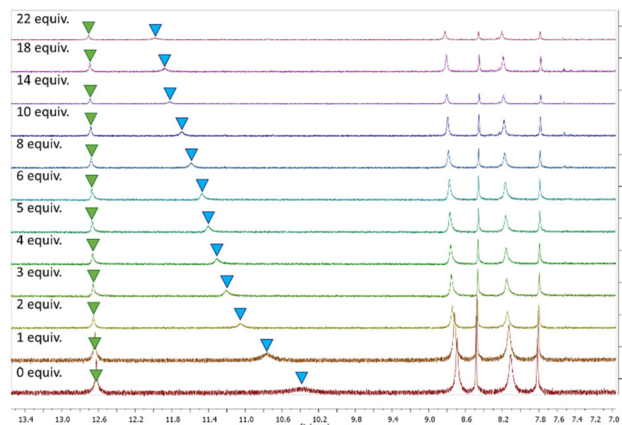


Fig. 4 ¹H NMR stackplot, 7.0–13.5 ppm, of receptor **3** with 0.0–22.0 equiv. TBACl in DMSO-*d*₆/0.5% H₂O.

Table 2 Summary of the binding constants for Cl⁻ (K_a/M^{-1}) of receptors **1–8** in 0.5% H₂O in DMSO-*d*₆ at 298 K, alongside error values and corresponding Hammett constants.²⁴ Data fitted to 1 : 1 binding model

Receptor	K_a/M^{-1}	% Error	<i>N</i> -amide p K_a (exp.)	Hammett constant
1	76	2.63	8.8	0.0 σ_p
2	97	3.58	7.3	0.54 σ_p
3	123	4.78	6.3	0.43 σ_m
4	54	2.85	7.5	0.78 σ_p
5	6	3.19	8.8	— ^a
6	52	1.85	8.1	0.18 σ_p
7	69	1.06	7.1	0.23 σ_p , 0.37 σ_m
8	58	1.47	8.2	0.23 σ_p

^a No Hammett constant reported for *o*-iodo substituent.

software BindFit^{27,28} (see ESI† for details), and fitted to a 1 : 1 binding model. The results are summarised in Table 2.

The binding affinity of the amidosquaramides were in the order of **3** > **2** > **1** > **7** > **8** > **4** \approx **6** > **5**. Unsurprisingly, compound **3** displayed the highest binding constant of 123 K_a/M^{-1} due to the presence of the bis-3,5-(trifluoro)methyl substituents on both aromatic rings. This aligns with previously reported receptors decorated with CF₃ moieties displaying the highest binding constants.²⁹ Compound **5** displayed the lowest binding constant of 6 K_a/M^{-1} . We postulate that this is a result of the 2-iodo substituent causing steric hindrance at the binding site, preventing Cl⁻ coming into close proximity with the NH hydrogen bond donor. When anion binding values are correlated with the appropriate Hammett parameter and p K_a values (Table 2) no clear trend emerges across the entire series. Some relationship is observed for compounds **1–3** where an increase in the Hammett constant results in a decrease in p K_a and an increase in anion binding affinity. However, this trend does not hold for receptors **4–8**.

When comparing amidosquaramides to analogous squaramides, ureas, and thioureas (Fig. 5a), we see that while amidosquaramides do not reach the anion binding ability of their analogous squaramides, they do show anion binding abilities



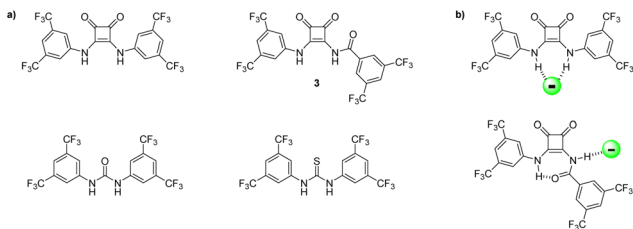


Fig. 5 (a) Structure of receptor **3**, alongside previously studied analogous squaramides, ureas, and thioureas.²⁹ (b) Comparison of binding modes of squaramide vs. amidosquaramide.

greater than that of their urea and thiourea analogues.²⁹ For example, amidosquaramide **3** displays a K_a value for Cl^- of 123 M^{-1} , while the binding constants for its analogous squaramide, urea, and thiourea are 643, 88, and $41 \text{ K}_a/\text{M}^{-1}$, respectively. We postulate that the *anti/syn* conformation of the receptors arising from the intramolecular H-bonding was a factor in the relatively low Cl^- binding constants, as only one hydrogen bond donor is available for H-bond formation with Cl^- , compared to the analogous squaramides where two hydrogen bond donors are available for anion binding (Fig. 5b).

Intramolecular H-bonds that affect anion binding are well known and several examples have been presented where the interactions can either favour the desired conformation^{30,31} that leads to increased anion binding or result in an undesired conformation that inhibits anion binding.³² For example, Jolliffe *et al.* recently showed this behaviour for diamino-methyleneindanediolines, where addition of SO_4^{2-} disrupted intramolecular H-bonding and led to enhanced binding. We expected that the intramolecular interaction of the amidosquaramides may be disrupted thereby promoting greater anion binding affinity. While DMSO is already a competitive H-bonding solvent we expected that the addition of acid would further increase the competitiveness and may lead to a disruption of the internal H-bond and, potentially, to a change in conformation. Therefore, we undertook a preliminary ^1H NMR study in the presence of camphor sulfonic acid (CSA) where we expected a conformational change may lead to variation in the ^1H NMR spectrum. Unfortunately, under our experimental conditions (100 equiv. CSA in a solution of **3** (2.5 mM) in $\text{DMSO}-d_6/0.5\% \text{H}_2\text{O}$; see ESI†) minimal changes were observed and suggested that no conformational change occurred. The experiment was repeated in the presence of both acetic acid (AcOH) and trifluoroacetic acid (TFA) under the same conditions but in each case, only minor shifts in the NMR were observed. These results suggest that the intramolecular H-bond is stable under very competitive environments and requires a significant amount of energy to 'reorganise' into the desired *anti/anti* conformation.

Anion transport studies

With just moderate Cl^- binding affinities, we expected that the amidosquaramides may not exhibit efficient anion transport as we had initially envisaged. Nevertheless, the anionophoric

activity of receptors **1–8** were screened using methods reported by Gale *et al.*³³ Briefly, unilamellar vesicles were created using a 7 : 3 molar ratio of 1-palmitoyl-2-oleoyl-sn-glycero-3-phosphocholine (POPC) and cholesterol with an internal environment of a NaCl solution (487 mM), buffered to pH 7.2 using a sodium phosphate buffer (5 mM). The liposomes were then purified by dialysis to suspend the vesicles in an isotonic external solution of NaNO_3 solution, buffered to pH 7.20 using a sodium phosphate buffer (5 mM). Using the external solution, the liposomes were diluted to 0.5 mM before each run was performed. The efflux of chloride was measured using a chloride ion selective electrode (ISE). The amidosquaramides were added to the vesicles as DMSO solutions *via* micropipette. See ESI† for detailed assay conditions.

Initially, the anionophoric activity of the amidosquaramides were assessed at pH 7.20 at a concentration of 5 mol% (with respect to POPC concentration), repeated in triplicate. The amidosquaramides were added at 0 seconds and the efflux was monitored for 300 seconds before the addition of a solution of Triton X-100 (11 wt% in H_2O : DMSO 7 : 1 v : v) in order to calibrate the 100% efflux value.

The results from the anion transport assays performed at pH 7.20 (Fig. 6a), revealed that the receptors displayed minimal transport at this pH. Receptor **2** demonstrated the most potent anionophoric activity, yet still failed to reach 50% efflux at 5 mol%. **4** and **5** also showed some activity, but to a lesser extent than **2**. The anionophoric activity of **2** is likely due to its relatively high binding affinity for Cl^- compared to the other receptors as well as its enhanced lipophilicity brought about by the trifluoromethyl substituents. However, while **3** displayed the highest binding constant and contained multiple trifluoromethyl moieties, which are known to increase lipophilicity and anion transport, the receptor was only able to facilitate approximately 20% Cl^- efflux.

The poor anion transport ability of the receptors, can be ascribed to a combination of the aforementioned intramolecular H-bonding in addition to their pK_a values that fall close to physiological pH. The range of pK_a values of the amidosquaramide amide NH were experimentally determined to be between 6.3–8.8. Thus, as the anion transport assays were performed at pH 7.20, a large proportion of the receptors would exist in their deprotonated state. As the amide NH is the only one available to participate in H-bonding, this effectively limits their ability to transport Cl^- at neutral pH. Such behaviour has previously been reported for thiosquaramides,²⁰ oxothiosquaramides,³⁴ and phenylthiosemicarbazones.³⁵

Therefore, the anion transport assays were repeated at pH 4.20, using the method described previously, with the solutions buffered to pH 4.20 using a citrate buffer. At acidic pH, a considerable increase was observed in the anionophoric activity of the amidosquaramides (Fig. 6b). **2** facilitated 100% Cl^- efflux at 5 mol%, and **4** also demonstrated a stark increase from approximately 30% efflux to approximately 80% efflux. The remaining receptors did not reach 50% efflux of Cl^- after 300 seconds, placing **2** and **4** as the most potent anionophores at this pH. Overall, these results established that amidosquara-



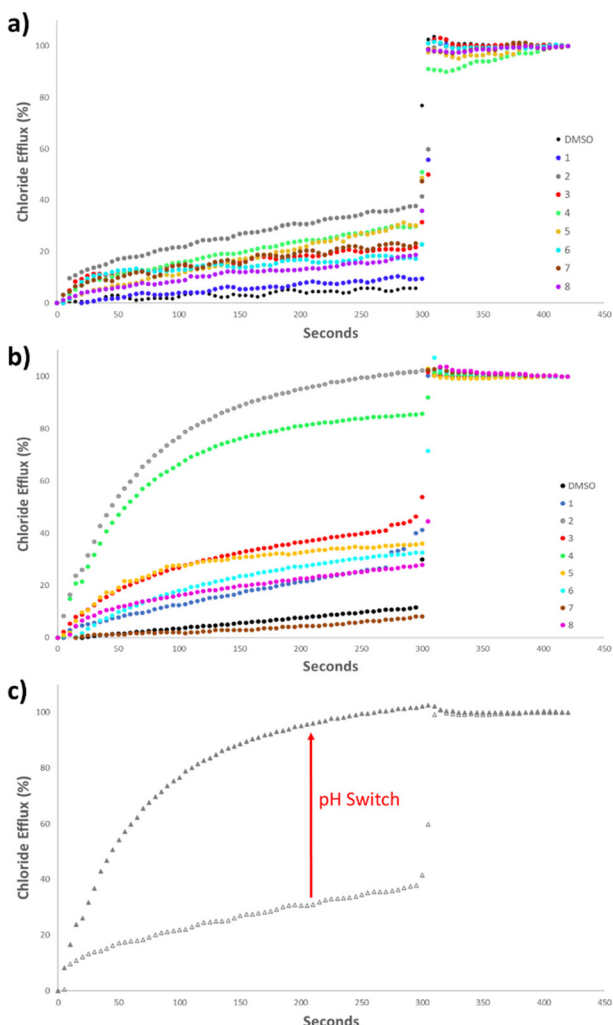


Fig. 6 (a) Chloride efflux facilitated by **1–8** (5 mol% receptor to lipid) from unilamellar POPC vesicles loaded with 487 mM NaCl, buffered to pH 7.20 with 5 mM sodium phosphate salts, suspended in 487 mM NaNO₃, buffered to pH 7.20 with 5 mM sodium phosphate salts. Each trace represents the average of three trials. (b) Chloride efflux facilitated by **1–8** (5 mol% receptor to lipid) from unilamellar POPC vesicles loaded with 487 mM NaCl, buffered to pH 4.20 with 5 mM citric acid buffer, and suspended in 487 mM NaNO₃, buffered to pH 4.20 with 5 mM citric acid buffer. Each trace represents the average of three trials. (c) Chloride efflux facilitated by **2** (5 mol%) at pH 7.2 (empty triangle) and at pH 4.2 (filled triangle).

mides can facilitate Cl[−]/NO₃[−] exchange across a lipid membrane, and display pH-switchable behaviour, where anion transport is ‘switched on’ at acidic pH. Gale and co-workers previously published a QSAR analysis of anion binding and transport where they found that the anion binding abilities of a family of thioureas are dominated by the pK_a of the thiourea NH.³⁶ The same work also showed that anion transport ability is mainly dependent on the lipophilicity of the transporter, the size of the transporter and the anion binding affinity. In short, it appears that the factors affecting anion transport are numerous and when dealing with receptors with a pK_a close to 7.4,

still poorly understood. We postulate that the observed ‘switch’ is either due to the protonation of the receptor at acidic pH or a switch in the conformation of the receptor at the lipid solvent interface (or a combination of both). Further investigation of this phenomenon is ongoing.

Conclusions

In conclusion, we have reported the syntheses of a small family of anion receptors that incorporate a new anion binding motif; amidosquaramides. We have shown, through a combination of experimental and computational methods that these receptors have pK_a values close to physiological pH but also display intramolecular H-bonding interactions. Both of these characteristics result in a decrease in binding affinity relative to their squaramide analogues but remain higher than those reported for analogous ureas and thioureas. The entire family of receptors were also screened for chloride transport ability where they showed moderate activity in a Cl[−]/NO₃[−] exchange assay at physiological pH, however, when experiments were repeated under acidic conditions, a significant increase in transport ability was observed. We suspect that the observed increase under acidic conditions is two-fold; brought about by a reprotonation of acidic NH's as well as a potential disruption of the intramolecular H-bonding (although we were unable to observe this experimentally). We are currently designing receptors containing amidosquaramides with a view to taking advantage of the intramolecular H-bond that could lead to a ‘conformational switch’. Such an advance should provide access to stimuli responsive anion transporters and our detailed investigations will be reported in due course.

Experimental

General experimental methods

All chemicals purchased were obtained from commercial suppliers and used without further purification. DCM was distilled over CaH₂ and MeCN was dried over 3 Å molecular sieves. Anhydrous DMF was purchased from Sigma Aldrich. TLC was performed on Merck Silica Gel F254 plates and visualised under UV light ($\lambda = 254$ nm). Flash chromatography was performed with Merck Silica Gel 60. Compounds were lyophilised on a Labconco Freezone 1 Dry system. NMR spectra were recorded on a Bruker Ascend 500 NMR spectrometer, operated at 500 MHz for ¹H NMR analysis and 126 MHz for ¹³C analysis, both at 293 K. The residual solvent peak was used as an internal standard for DMSO-*d*₆ and (CD₃)₂CO and TMS for CDCl₃. Chemical shifts (δ) were reported in ppm. NMR spectra were processed and stack plots produced using MestReNova 6.0.2 software. Proton and carbon signals were assigned with the aid of 2D NMR experiments (COSY, HSQC and HMBC). Multiplicity is given as s = singlet, bs = broad singlet, d = doublet, brd = broad doublet, dd = doublet of doublets, ddd = doublet of doublet of doublets, t = triplet, q = quartet, m =



multiplet as appropriate, and J values are given in Hz. Infrared spectra were obtained *via* ATR as a solid on a zinc selenide crystal in the region of 4000–400 cm^{-1} on a PerkinElmer Spectrum 100 FT-IR spectrophotometer. LC-MS was performed on an Agilent Technologies 1200 Series instrument consisting of a G1322A Quaternary pump and a G1314B UV detector (254 nm) coupled to an Advion Expression L Compact Mass spectrometer (ESI) operating in positive mode. High resolution ESI spectra were recorded on an Agilent 6310 LCMS TOF. UV-vis spectra were recorded on a Varian Cary 50 Scan UV-visible spectrophotometer using Cary WinUV software. pH measurements were recorded using a Jenway 350 pH meter. Conductivity measurements were performed using an Orion Star A211 Benchtop pH Meter and a Fisherbrand accumet chloride combination electrode.

3,4-Diethoxy-3-cyclobutene-1,2-dione (9). 3,4-Diethoxy-3-cyclobutene-1,2-dione was synthesised following methods previously reported by Moore *et al.*¹⁸ 3,4-Dihydroxy-3-cyclobutene-1,2-dione (6 g, 53 mmol) was suspended in EtOH (150 mL). Triethyl orthoformate (21.5 mL, 145 mmol) was added to the suspension and refluxed for 72 hours. The solvent was removed *in vacuo* and the resulting oil was purified *via* column chromatography (DCM) to yield the product as a yellow oil (8.5 g, 94%). ^1H NMR (500 MHz, DMSO- d_6) δ 4.63 (q, J = 7.1 Hz, 1H), 1.35 (t, J = 7.1 Hz, 2H). ^{13}C NMR (126 MHz, DMSO- d_6) δ 189.6 (s), 184.2 (s), 70.8 (s), 15.7 (s). IR (ATR): ν_{max} (cm^{-1}) = 2986, 1811, 1730, 1592, 1482, 1421, 1330, 1187 cm^{-1} . HRMS (ESI $^+$): m/z calcd for $\text{C}_{13}\text{H}_{11}\text{NO}_4$ 246.0688 [M + H] $^+$, found 246.0764.

3-Amino-4-ethoxy-3-cyclobutene-1,2-dione (10). 3-Amino-4-ethoxy-3-cyclobutene-1,2-dione was synthesised using adapted methods previously reported by Davis *et al.*¹² 3,4-Diethoxy-3-cyclobutene-1,2-dione (4.5 g, 26.5 mmol) was dissolved in EtOH (100 mL). 2M Ammonia in ethanol solution (13.5 mL, 26.5 mmol) was added portion-wise over 6 hours. Upon completion of the addition, the reaction was left to stir overnight (approx. 18 hours) at room temperature. The reaction mixture was filtered and the filtrate was concentrated *in vacuo* to yield a beige solid. Diethyl ether (100 mL) was added to the flask to create a suspension, after which the flask was sonicated for a period of 15 minutes. The suspension was then filtered, washed with diethyl ether and dried *via* vacuum filtration to yield the product as a pale yellow solid (2.6 g, 70%). ^1H NMR (500 MHz, DMSO- d_6) δ 8.33 (brd, J = 68.0 Hz, 2H), 4.63 (q, J = 7.1 Hz, 2H), 1.36 (t, J = 7.1 Hz, 3H). ^{13}C NMR (126 MHz, DMSO- d_6) δ 190.5, 183.5, 178.2, 174.8, 69.0, 16.1. IR (ATR): ν_{max} (cm^{-1}) = 3332, 3074, 1810, 1700, 1641, 1547, 1435, 1350, 1261, 1032, 873, 773. HRMS (ESI $^+$): m/z calcd for $\text{C}_6\text{H}_7\text{NO}_3$ 142.0499 [M + H] $^+$, found 142.0501.

N-(2-Ethoxy-3,4-dioxocyclobut-1-en-1-yl) benzamide (11). Benzoic acid (394 mg, 3.22 mmol), 4-dimethylaminopyridine (433 mg, 3.54 mmol) and 1-ethyl-3-(3-dimethylaminopropyl) carbodiimide (678 mg, 3.54 mmol) were placed under a N_2 atmosphere and dissolved in anhydrous MeCN (20 mL) and stirred for 15 minutes. 3-Amino-4-ethoxy-3-cyclobutene-1,2-dione (500 mg, 3.54 mmol) was placed under N_2 atmosphere and dissolved in anhydrous MeCN (20 mL) and transferred to the reaction flask *via* cannulation. The reaction was left to stir

overnight (approx. 18 hours) at room temperature. The solvent was removed using a rotary evaporator and the obtained white solid was purified by column chromatography (SiO₂, 10% MeCN in DCM) to yield an off-white solid (600 mg, 76%). ^1H NMR (500 MHz, CDCl₃) δ 9.88 (s, 1H), 8.03 (dd, J = 8.3, 1.1 Hz, 2H), 7.64–7.59 (m, 1H), 7.51 (dd, J = 11.6, 4.2 Hz, 2H), 4.95 (q, J = 7.1 Hz, 2H), 1.54 (t, J = 7.1 Hz, 3H). ^{13}C NMR (126 MHz, CDCl₃) δ 188.7, 188.6, 184.9, 167.00, 163.50, 133.8, 131.1, 129.00, 128.5, 71.2, 15.9. IR (ATR): ν_{max} (cm^{-1}) = 3305, 3001, 1814, 1707, 1581, 1519, 1340, 1250, 1125, 1060, 1006, 865. HRMS (ESI $^+$): m/z calcd for $\text{C}_{13}\text{H}_{11}\text{NO}_4$ 246.0688 [M + H] $^+$, found 246.0764.

N-(2-Ethoxy-3,4-dioxocyclobut-1-en-1-yl)-4-(trifluoromethyl) benzamide (12). 4-(Trifluoromethyl) benzoic acid (612 mg, 3.22 mmol), 4-dimethylaminopyridine (433 mg, 3.54 mmol) and 1-ethyl-3-(3-dimethylaminopropyl) carbodiimide (678 mg, 3.54 mmol) were placed under a N_2 atmosphere and dissolved in anhydrous MeCN (20 mL) and stirred for 15 minutes. 3-Amino-4-ethoxy-3-cyclobutene-1,2-dione (500 mg, 3.54 mmol) was placed under N_2 atmosphere and dissolved in anhydrous MeCN (20 mL) and transferred to the reaction flask *via* cannulation. The reaction was left to stir overnight (approx. 18 hours) at room temperature. The solvent was removed using a rotary evaporator and the obtained white solid was purified by column chromatography (SiO₂, 15% MeCN in DCM) to yield an off-white solid (540 mg, 54%). ^1H NMR (500 MHz, DMSO- d_6) δ 12.17 (s, 1H), 8.19 (d, J = 8.1 Hz, 2H), 7.92 (d, J = 8.2 Hz, 2H), 4.82 (q, J = 7.1 Hz, 2H), 1.42 (t, J = 7.1 Hz, 3H). ^{13}C NMR (126 MHz, DMSO) δ 190.6, 187.4, 185.0, 169.0, 163.4, 135.9, 133.00 (q, $^2J_{\text{CF}}$ = 32.0 Hz), 130.3, 125.9 (overlapping signals X 3), 124.2 (q, $^1J_{\text{CF}}$ = 273.4 Hz), 70.6, 16.0. IR (ATR): ν_{max} (cm^{-1}) = 3295, 2986, 1813, 1707, 1581, 1525, 1411, 1326, 1260, 1129, 1059, 1004, 854, 755. HRMS (ESI $^+$): m/z calcd for $\text{C}_{14}\text{H}_{10}\text{F}_3\text{NO}_4$ [M + H] $^+$ 314.0562, found 314.0637.

N-(2-Ethoxy-3,4-dioxocyclobut-1-en-1-yl)-3,5-bis(trifluoromethyl) benzamide (13). Bis-3,5-(trifluoromethyl) benzoic acid (831 mg, 3.22 mmol), 4-dimethylaminopyridine (433 mg, 3.54 mmol) and 1-ethyl-3-(3-dimethylaminopropyl) carbodiimide (678 mg, 3.54 mmol) were placed under a N_2 atmosphere and dissolved in anhydrous MeCN (30 mL) and stirred for 15 minutes. 3-Amino-4-ethoxy-3-cyclobutene-1,2-dione (500 mg, 3.54 mmol) was placed under N_2 atmosphere and dissolved in anhydrous MeCN (20 mL) and transferred to the reaction flask *via* cannulation. The reaction was left to stir overnight (approx. 18 hours) at room temperature. The solvent was removed using a rotary evaporator and the obtained white solid was purified by column chromatography (SiO₂, 20% MeCN in DCM) to yield an off-white solid (504 mg, 41%). ^1H NMR (500 MHz, DMSO- d_6) δ 12.38 (s, 1H), 8.65 (s, 2H), 8.44 (s, 1H), 4.83 (q, J = 7.1 Hz, 2H), 1.42 (t, J = 7.1 Hz, 3H). ^{13}C NMR (126 MHz, DMSO) δ 190.5, 187.4, 185.1, 168.6, 161.7, 131 (q, $^2J_{\text{CF}}$ = 33.5 Hz), 130.2 (overlapping C X 2), 126.7 (overlapping C X 2), 123.4 (q, $^1J_{\text{CF}}$ = 273.1 Hz), 70.8, 16.0. IR (ATR): ν_{max} (cm^{-1}) = 3282, 3195, 3037, 1807, 1736, 1601, 1530, 1353, 1272, 1131, 992, 901, 817, 757. HRMS (ESI $^+$): m/z calcd for $\text{C}_{15}\text{H}_9\text{F}_6\text{NO}_4$ [M + H] $^+$ 382.0436, found 382.0510.



N-(2-Ethoxy-3,4-dioxocyclobut-1-en-1-yl)-4-nitrobenzamide (14). 4-Nitrobenzoic acid (538 mg, 3.22 mmol), 4-dimethylaminopyridine (433 mg, 3.54 mmol) and 1-ethyl-3-(3-dimethylaminopropyl) carbodiimide (678 mg, 3.54 mmol) were placed under a N_2 atmosphere and dissolved in anhydrous DMF (40 mL) and stirred for 15 minutes. 3-Amino-4-ethoxy-3-cyclobutene-1,2-dione (500 mg, 3.54 mmol) was placed under N_2 atmosphere and dissolved in anhydrous MeCN (20 mL) and transferred to the reaction flask *via* cannulation. The reaction was left to stir overnight (approx. 18 hours) at room temperature. The solvent was removed using a rotary evaporator and the obtained yellow solid was purified by column chromatography (SiO_2 , 20% MeCN in DCM) to yield a yellow solid (504 mg, 41%). **$^1\text{H NMR}$** (500 MHz, $\text{DMSO}-d_6$) δ 12.26 (s, 1H), 8.36 (d, J = 8.8 Hz, 2H), 8.22 (d, J = 8.7 Hz, 2H), 4.83 (q, J = 7.1 Hz, 2H), 1.42 (t, J = 7.1 Hz, 3H). **$^{13}\text{C NMR}$** (126 MHz, $\text{DMSO}-d_6$) δ 190.6, 187.4, 185.1, 168.9, 162.9, 150.4, 137.7, 130.9, 124.0, 70.7, 16.0. **IR (ATR):** ν_{max} (cm^{-1}) = 3295, 1814, 1707, 1582, 1525, 1412, 1327, 1255, 1133, 980, 853, 775, 712. **HRMS (ESI+)** m/z calcd for $\text{C}_{13}\text{H}_{10}\text{N}_2\text{O}_6$ $[\text{M} + \text{H}]^+$ 291.0539, found 291.0613.

N-(2-Ethoxy-3,4-dioxocyclobut-1-en-1-yl)-2-iodobenzamide (15). 2-Iodoobenzoic acid (800 mg, 3.22 mmol), 4-dimethylaminopyridine (433 mg, 3.54 mmol) and 1-ethyl-3-(3-dimethylaminopropyl) carbodiimide (678 mg, 3.54 mmol) were placed under a N_2 atmosphere and dissolved in anhydrous MeCN (30 mL) and stirred for 15 minutes. 3-Amino-4-ethoxy-3-cyclobutene-1,2-dione (500 mg, 3.54 mmol) was placed under N_2 atmosphere and dissolved in anhydrous MeCN (20 mL) and transferred to the reaction flask *via* cannulation. The reaction was left to stir overnight (approx. 18 hours) at room temperature. The solvent was removed using a rotary evaporator and the obtained off-white solid was purified by column chromatography (SiO_2 , 15% MeCN in DCM) to yield a white solid (358 mg, 30%). **$^1\text{H NMR}$** (500 MHz, $\text{DMSO}-d_6$) δ 12.09 (s, 1H), 7.95 (dd, J = 7.9, 0.7 Hz, 1H), 7.57–7.46 (m, 3H), 7.27 (ddd, J = 7.9, 7.1, 2.0 Hz, 1H), 4.80 (q, J = 7.1 Hz, 2H), 1.41 (t, J = 7.1 Hz, 3H). **$^{13}\text{C NMR}$** (126 MHz, DMSO) δ 190.3, 187.2, 184.7, 168.4, 166.3, 140.3, 139.8, 132.6, 129.5, 128.5, 94.1, 70.6, 16.0. **IR (ATR):** ν_{max} (cm^{-1}) = 3246, 3192, 1809, 1723, 1700, 1606, 1575, 1507, 1484, 1421, 1286, 1239, 1123, 1137, 1103, 957, 935, 901, 848, 784, 749, 703. **HRMS (ESI+)** m/z calcd for $\text{C}_{13}\text{H}_{10}\text{INO}_4$ $[\text{M} + \text{H}]^+$ 371.9655, found 371.9728.

N-(2-Ethoxy-3,4-dioxocyclobut-1-en-1-yl)-4-iodobenzamide (16). 2-Iodoobenzoic acid (800 mg, 3.22 mmol), 4-dimethylaminopyridine (433 mg, 3.54 mmol) and 1-ethyl-3-(3-dimethylaminopropyl) carbodiimide (678 mg, 3.54 mmol) were placed under a N_2 atmosphere and dissolved in anhydrous MeCN (30 mL) and stirred for 15 minutes. 3-Amino-4-ethoxy-3-cyclobutene-1,2-dione (500 mg, 3.54 mmol) was placed under N_2 atmosphere and dissolved in anhydrous MeCN (20 mL) and transferred to the reaction flask *via* cannulation. The reaction was left to stir overnight (approx. 18 hours) at room temperature. The solvent was removed using a rotary evaporator and the obtained off-white solid was purified by column chromatography (SiO_2 , 15% MeCN in DCM) to yield a white solid (600 mg, 50%). **$^1\text{H NMR}$** (500 MHz, $\text{DMSO}-d_6$) δ 11.99 (s, 1H),

11.99 (s, 1H), 7.95–7.91 (m, 2H), 7.79–7.75 (m, 2H), 4.81 (q, J = 7.1 Hz, 2H), 4.81 (q, J = 7.1 Hz, 2H), 1.41 (t, J = 7.1 Hz, 3H), 1.41 (t, J = 7.1 Hz, 3H). **$^{13}\text{C NMR}$** (126 MHz, $\text{DMSO}-d_6$) δ 190.5, 187.5, 184.9, 169.3, 163.8, 138.0, 131.5, 131.1, 102.1, 70.6, 161. **IR (ATR):** ν_{max} (cm^{-1}) = 3296, 1812, 1732, 1707, 1576, 1515, 1480, 1408, 1377, 1328, 1256, 1058, 997, 836, 742. **HRMS (ESI+)** m/z calcd for $[\text{M} + \text{H}]^+$ 371.9655, found 371.9727.

3,4-Dichloro-N-(2-ethoxy-3,4-dioxocyclobut-1-en-1-yl)benzamide (17). 3,4-Dichlorobenzoic acid (612 mg, 3.22 mmol), 4-dimethylaminopyridine (433 mg, 3.54 mmol) and 1-ethyl-3-(3-dimethylaminopropyl) carbodiimide (678 mg, 3.54 mmol) were placed under a N_2 atmosphere and dissolved in anhydrous MeCN (30 mL) and stirred for 15 minutes. 3-Amino-4-ethoxy-3-cyclobutene-1,2-dione (500 mg, 3.54 mmol) was placed under N_2 atmosphere and dissolved in anhydrous MeCN (20 mL) and transferred to the reaction flask *via* cannulation. The reaction was left to stir overnight (approx. 18 hours) at room temperature. The solvent was removed using a rotary evaporator and the obtained yellow solid was purified by column chromatography (SiO_2 , 15% MeCN in DCM) to yield an off-white solid (539 mg, 54%). **$^1\text{H NMR}$** (500 MHz, $\text{DMSO}-d_6$) δ 12.12 (s, 1H), 8.31 (d, J = 2.1 Hz, 1H), 7.96 (dd, J = 8.4, 2.1 Hz, 1H), 7.84 (d, J = 8.4 Hz, 1H), 4.82 (q, J = 7.1 Hz, 2H), 1.42 (t, J = 7.1 Hz, 3H). **$^{13}\text{C NMR}$** (126 MHz, $\text{DMSO}-d_6$) δ 190.5, 187.4, 185.0, 169.0, 162.2, 136.4, 132.5, 131.9, 131.4, 131.2, 129.6, 70.6, 16.0. **IR (ATR):** ν_{max} (cm^{-1}) = 3293, 1807, 1702, 1580, 1517, 1468, 1406, 1334, 1256, 1132, 1064, 984, 907, 851, 750. **HRMS (ESI+)** m/z calcd for $\text{C}_{13}\text{H}_9\text{Cl}_2\text{NO}_4$ $[\text{M} + \text{H}]^+$ 313.9909, found 313.9982.

4-Chloro-N-(2-ethoxy-3,4-dioxocyclobut-1-en-1-yl)benzamide (18). 4-Chlorobenzoic acid (503 mg, 3.22 mmol), 4-dimethylaminopyridine (433 mg, 3.54 mmol) and 1-ethyl-3-(3-dimethylaminopropyl) carbodiimide (678 mg, 3.54 mmol) were placed under a N_2 atmosphere and dissolved in anhydrous MeCN (30 mL) and stirred for 15 minutes. 3-Amino-4-ethoxy-3-cyclobutene-1,2-dione (500 mg, 3.54 mmol) was placed under N_2 atmosphere and dissolved in anhydrous MeCN (20 mL) and transferred to the reaction flask *via* cannulation. The reaction was left to stir overnight (approx. 18 hours) at room temperature. The solvent was removed using a rotary evaporator and the obtained off-white solid was purified by column chromatography (SiO_2 , 15% MeCN in DCM) to yield a white solid (458 mg, 51%). **$^1\text{H NMR}$** (500 MHz, CDCl_3) δ 12.04 (s, 1H), 8.05–8.00 (m, 2H), 7.64–7.60 (m, 2H), 4.81 (q, J = 7.1 Hz, 2H), 1.41 (t, J = 7.1 Hz, 3H). **$^{13}\text{C NMR}$** (126 MHz, CDCl_3) δ 190.0, 187.1, 184.4, 168.8, 162.9, 138.1, 130.8, 130.4, 128.7, 70.1, 15.6. **IR (ATR):** ν_{max} (cm^{-1}) = 3682, 3291, 2973, 2866, 1815, 1707, 1579, 1485, 1411, 1323, 1256, 1056, 855, 750. **HRMS (ESI+)** m/z calcd for $\text{C}_{13}\text{H}_{10}\text{ClNO}_4$ $[\text{M} + \text{H}]^+$ 280.0298, found 280.0370.

N-(3,4-Dioxo-2-(phenylamino)cyclobut-1-en-1-yl)benzamide (1). *N*-(2-Ethoxy-3,4-dioxocyclobut-1-en-1-yl) benzamide (200 mg, 0.82 mmol) and zinc trifluoromethanesulfonate (58 mg, 0.16 mmol) were dissolved in MeCN (40 mL) and stirred for 5 minutes. Aniline (90 μL , 0.98 mmol) was added to the solution and stirred for 1 hour at room temperature. The precipitate was filtered and washed with MeCN to yield the product as a pale yellow solid. **$^1\text{H NMR}$** (500 MHz, $\text{DMSO}-d_6$) δ 11.95 (s,



1H), 9.98 (s, 1H), 8.07 (d, J = 5.9 Hz, 2H), 7.68 (t, J = 7.4 Hz, 1H), 7.57 (t, J = 7.7 Hz, 2H), 7.42 (s, 2H), 7.38 (t, J = 7.1 Hz, 2H), 7.14 (t, J = 7.0 Hz, 1H). ^{13}C NMR (126 MHz, DMSO- d_6) δ 188.0, 183.1, 171.0, 166.0, 163.7, 138.0, 133.7, 132.3, 129.5, 129.4, 129.1, 124.8, 120.67. IR (ATR): ν_{max} (cm $^{-1}$) = 3227, 1809, 1724, 1588, 1504, 1392, 1275, 1155, 897, 751. HRMS (ESI $^+$) m/z calcd for $\text{C}_{17}\text{H}_{12}\text{N}_2\text{O}_3$ [M + H] $^+$ 293.0848, found 293.0926.

N-(3,4-Dioxo-2-((4-(trifluoromethyl)phenyl)amino)cyclobut-1-en-1-yl)-4-(trifluoromethyl)benzamide (2). N -(2-Ethoxy-3,4-dioxocyclobut-1-en-1-yl)-4-(trifluoromethyl)benzamide (200 mg, 0.64 mmol) and zinc trifluoromethanesulfonate (48 mg, 0.13 mmol) were dissolved in MeCN (40 mL) and stirred for 5 minutes. 4-Trifluoroaniline (97 μL , 0.77 mmol) was added to the solution and refluxed overnight (approximately 18 hours). The solvent was removed *in vacuo* to yield a pale yellow solid. The crude product was purified using column chromatography (SiO₂, 10% MeCN in DCM) to yield a yellow solid (164 mg, 60%). ^1H NMR (500 MHz, DMSO- d_6) δ 12.26 (s, 1H), 10.24 (s, 1H), 8.24 (d, J = 7.7 Hz, 2H), 7.96 (d, J = 7.9 Hz, 2H), 7.72 (d, J = 8.0 Hz, 2H), 7.60 (d, J = 7.2 Hz, 2H). ^{13}C NMR (126 MHz, DMSO- d_6) δ 188.1, 183.8, 171.40, 164.7, 163.8, 141.5, 135.9, 133.1 (q, $^2J_{\text{CF}}$ = 32.2 Hz), 130.2, 126.7, 126.0, 124.8 (q, $^1J_{\text{CF}}$ = 277.2 Hz), 124.2 (q, $^1J_{\text{CF}}$ = 277.2 Hz) 120.8. IR (ATR): ν_{max} (cm $^{-1}$) = 3234, 3196, 3181, 1727, 2581, 1545, 1382, 1319, 1273, 1112, 835, 700. HRMS (ESI $^+$) m/z calcd for $\text{C}_{19}\text{H}_{10}\text{F}_6\text{N}_2\text{O}_3$ [M + H] $^+$ 428.0596, found 429.0926.

N-(2-((3,5-Bis(trifluoromethyl)phenyl)amino)-3,4-dioxocyclobut-1-en-1-yl)-3,5-bis(trifluoromethyl)benzamide (3). N -(2-Ethoxy-3,4-dioxocyclobut-1-en-1-yl)-3,5-bis(trifluoromethyl)benzamide (250 mg, 0.66 mmol) and zinc trifluoromethanesulfonate (48 mg, 0.13 mmol) were dissolved in MeCN (40 mL) and stirred for 5 minutes. 4-Trifluoroaniline (123 μL , 0.78 mmol) was added to the solution and refluxed overnight (approximately 18 hours). The solvent was removed *in vacuo* to yield an off-white solid. The crude product was purified using column chromatography (SiO₂, 10% MeCN in DCM) to yield an off-white solid (100 mg, 33%). ^1H NMR (500 MHz, Acetone- d_6) δ 11.56 (s, 1H), 10.21 (s, 1H), 8.80 (s, 2H), 8.43 (s, 1H), 8.28 (s, 2H), 7.80 (d, J = 0.5 Hz, 1H). ^{13}C NMR (126 MHz, Acetone- d_6) δ 186.79, 182.58, 170.66, 164.20, 162.32, 139.62, 134.08, 131.9 (m/overlapping quartets X 2, $^2J_{\text{CF}}$ = 25 Hz), 129.5 (overlapping C X 2), 126.8 (m/overlapping quartets X 2, $^3J_{\text{CF}}$ = 4 Hz), 123.4 (q, $^1J_{\text{CF}}$ = 270 Hz), 123.1 (q, $^1J_{\text{CF}}$ = 271 Hz), 120.7 (overlapping C X 2), 170.1, 119.9 117.2 (m/overlapping quartets, $^3J_{\text{CF}}$ = 4 Hz). IR (ATR): ν_{max} (cm $^{-1}$) = 3234, 1809, 1728, 1683, 1608 1585, 1530, 1477, 1376, 1290, 1273, 1233, 1135, 1033, 856, 824, 129. HRMS (ESI $^+$) m/z calcd for $\text{C}_{21}\text{H}_{18}\text{F}_{12}\text{N}_2\text{O}_3$ [M + H] $^+$ 428.0343, found 565.0414.

4-Nitro-N-(2-((4-nitrophenyl)amino)-3,4-dioxocyclobut-1-en-1-yl)benzamide (4). N -(2-Ethoxy-3,4-dioxocyclobut-1-en-1-yl)-4-nitrobenzamide (292 mg, 1 mmol) and zinc trifluoromethanesulfonate (72 mg, 0.2 mmol) were dissolved in MeCN (40 mL) and stirred for 5 minutes. 4-Nitroaniline (152 mg, 1.1 mmol) was added to the solution and refluxed overnight (approximately 18 hours). The precipitate was filtered and washed with hot MeCN to yield the product as a yellow solid (42 mg, 11%). ^1H

NMR (500 MHz, DMSO- d_6) δ 12.44 (s, 1H), 10.44 (s, 1H), 8.40 (d, J = 8.8 Hz, 2H), 8.26 (t, J = 8.6 Hz, 4H), 7.62 (d, J = 8.9 Hz, 2H). ^{13}C NMR (126 MHz, DMSO) δ 188.1, 184.2, 171.3, 164.4, 164.2, 150.5, 144.1, 143.4, 137.6, 130.9, 125.6, 124.2, 120.4. IR (ATR): ν_{max} (cm $^{-1}$) = 3234, 1809, 1728, 1683, 1608 1585, 1530, 1477, 1376, 1290, 1273, 1233, 1135, 1033, 856, 824, 729. HRMS (ESI $^+$) m/z calcd for $\text{C}_{17}\text{H}_{10}\text{N}_4\text{O}_7$ [M + H] $^+$ 382.0544, found 353.0626.

2-Iodo-N-(2-((2-iodophenyl)amino)-3,4-dioxocyclobut-1-en-1-yl)benzamide (5). N -(2-Ethoxy-3,4-dioxocyclobut-1-en-1-yl)-2-iodobenzamide (200 mg, 0.54 mmol) and zinc trifluoromethanesulfonate (40 mg, 0.11 mmol) were dissolved in MeCN (40 mL) and stirred for 5 minutes. 2-Iodoaniline (130 mg, 0.59 mmol) was added to the solution and refluxed overnight (approximately 18 hours). The precipitate was filtered and washed with hot MeCN to yield the product as an off-white solid (106 mg, 36%). ^1H NMR (500 MHz, DMSO) δ 12.48 (s, 1H), 9.88 (s, 1H), 7.98 (dd, J = 7.9, 0.8 Hz, 1H), 7.90 (dt, J = 3.4, 1.7 Hz, 1H), 7.66–7.60 (m, J = 11.5, 2.6 Hz, 2H), 7.54 (td, J = 7.5, 1.1 Hz, 1H), 7.46–7.41 (m, J = 8.1, 7.5, 1.4 Hz, 1H), 7.29 (td, 1H), 6.98 (td, 1H). ^{13}C NMR (126 MHz, DMSO) δ 187.1, 183.3, 170.6, 169.2, 162.7, 140.0, 139.8, 139.5, 138.6, 132.7, 129.4, 128.5, 127.4, 123.2, 94.2, 91.9. IR (ATR): ν_{max} (cm $^{-1}$) = 3246, 3192, 1809, 1723, 1700, 1606, 1575, 1507, 1484, 1421, 1286, 1239, 1153, 1137, 1103, 1017, 901, 750, 703. HRMS (ESI $^+$) m/z calcd for $\text{C}_{17}\text{H}_{10}\text{I}_2\text{N}_2\text{O}_3$ [M + H] $^+$ 544.8781, found 544.8851.

4-Iodo-N-(2-((4-iodophenyl)amino)-3,4-dioxocyclobut-1-en-1-yl)benzamide (6). N -(2-Ethoxy-3,4-dioxocyclobut-1-en-1-yl)-4-iodobenzamide (200 mg, 0.72 mmol) and zinc trifluoromethanesulfonate (40 mg, 0.11 mmol) were dissolved in MeCN (40 mL) and stirred for 5 minutes. 4-Iodoaniline (130 mg, 0.59 mmol) was added to the reaction mixture and refluxed overnight (approximately 18 hours). The precipitate was filtered and washed with hot MeCN to yield the product as an off-white solid (150 mg, 51%). ^1H NMR (500 MHz, DMSO- d_6) δ 12.03 (s, 1H), 9.95 (s, 1H), 7.97 (d, J = 8.5 Hz, 2H), 7.81 (d, J = 7.7 Hz, 2H), 7.70 (d, J = 8.3 Hz, 2H), 7.24 (s, 2H). ^{13}C NMR (126 MHz, DMSO) δ 165.2, 138.1, 138.0, 137.9, 131.6, 131.1, 123.1, 102.2, 89.1. IR (ATR): ν_{max} (cm $^{-1}$) = 3221, 3178, 1813, 1791, 1606, 1574, 1529, 1488, 1374, 1273, 1156, 1127, 1004, 899, 812, 733. HRMS (ESI $^+$) m/z calcd for $\text{C}_{17}\text{H}_{10}\text{I}_2\text{N}_2\text{O}_3$ [M + H] $^+$ 544.8781, found 544.8851.

3,4-Dichloro-N-(2-((3,4-dichlorophenyl)amino)-3,4-dioxocyclobut-1-en-1-yl)benzamide (7). 3,4-Dichloro- N -(2-ethoxy-3,4-dioxocyclobut-1-en-1-yl)benzamide (235 mg, 0.75 mmol) and zinc trifluoromethanesulfonate (55 mg, 0.15 mmol) were dissolved in MeCN (40 mL) and stirred for 5 minutes. 3,4-Dichloroaniline (145 mg, 0.9 mmol) was added to the reaction mixture and refluxed overnight (approximately 18 hours). The precipitate was filtered and washed with hot MeCN to yield the product as a pale yellow solid (170 mg, 53%). ^1H NMR (500 MHz, DMSO- d_6) δ 12.21 (s, 1H), 10.21 (s, 1H), 8.34 (s, 1H), 8.01 (d, J = 7.2 Hz, 1H), 7.86 (d, J = 8.4 Hz, 1H), 7.77 (s, 1H), 7.61 (d, J = 8.7 Hz, 1H), 7.39 (d, J = 7.6 Hz, 1H). ^{13}C NMR (126 MHz, DMSO- d_6) δ 131.9, 131.7, 131.4, 131.2, 129.5 IR (ATR): ν_{max} (cm $^{-1}$) = 3168, 3113, 3078, 3057, 2990, 1813, 1738,



1619, 1575, 1517, 1374, 1325, 1270, 1106, 852, 748, 708. **HRMS** (ESI+) m/z calcd for $C_{17}H_8Cl_4N_2O_3$ [M – H][–] 426.9289, found 426.9213.

4-Chloro-N-(2-((4-chlorophenyl)amino)-3,4-dioxocyclobut-1-en-1-yl)benzamide (8). 4-Chloro-N-(2-ethoxy-3,4-dioxocyclobut-1-en-1-yl)benzamide (200 mg, 0.72 mmol) and zinc trifluoromethanesulfonate (52 mg, 0.14 mmol) were dissolved in MeCN (40 mL) and stirred for 5 minutes. 4-Chloroaniline (109 mg, 0.86 mmol) was added to the reaction mixture and refluxed overnight (approximately 18 hours). The precipitate was filtered and washed with hot MeCN to yield the product as a pale yellow solid (109 mg, 42%). **¹H NMR** (500 MHz, DMSO-*d*₆) δ 12.06 (s, 1H), 9.96 (s, 1H), 8.07 (d, *J* = 7.7 Hz, 2H), 7.65 (d, *J* = 8.6 Hz, 2H), 7.42 (s, 4H). **¹³C NMR** (126 MHz, DMSO-*d*₆) δ 188.0, 183.4, 171.0, 164.8, 163.3, 138.6, 137.0, 131.2, 131.0, 129.3, 129.2, 129.0, 122.6. **IR** (ATR): ν_{max} (cm^{–1}) = 2973, 2950, 1809, 1724, 1579, 1487, 1455, 1371, 1265, 1057, 1034, 1011, 899, 841, 816, 745. **HRMS** (ESI+) m/z calcd for $C_{17}H_{10}Cl_2N_2O_3$ [M + Na]⁺ 383.0068, found 382.9960.

Author contributions

RE, LM and TK designed the study and wrote the manuscript. RE and TK supervised the study. LM synthesized and characterized the compounds and carried out spectroscopic titrations and anion transport assays. TK conducted computational calculations. All authors discussed the results and commented on the manuscript.

Conflicts of interest

There are no conflicts to declare.

Acknowledgements

L. M. acknowledges Maynooth University for a Hume Scholarship. R. E. and L. M. acknowledges funding from Science Foundation Ireland (SFI), grant number 12/RC/2275/P2, which is co-funded under the European Regional Development Fund. SFI are also acknowledged for the funding of the NMR facility (12/RI/2346/SOF) through the Research Infrastructure Programme and the Advion Compact Mass Spec through the Opportunistic Infrastructure Fund (16/RI/3399). T. K. wishes to acknowledge the DJEI/DES/SFI/HEA Irish Centre for High-End Computing (ICHEC) for the provision of computational facilities and support.

Notes and references

- 1 L. A. Marchetti, L. K. Kumawat, N. Mao, J. C. Stephens and R. B. P. Elmes, *Chem.*, 2019, **5**, 1398–1485.
- 2 Y. Li, G.-H. Yang, Y.-Y. Shen, X.-S. Xue, X. Li and J.-P. Cheng, *J. Org. Chem.*, 2017, **82**, 8662–8667.

- 3 D. Quiñonero, A. Frontera, G. A. Suñer, J. Morey, A. Costa, P. Ballester and P. M. Deyà, *Chem. Phys. Lett.*, 2000, **326**, 247–254.
- 4 L. K. Kumawat, A. A. Abogunrin, M. Kickham, J. Pardeshi, O. Fenelon, M. Schroeder and R. B. P. Elmes, *Front. Chem.*, 2019, **7**, 354.
- 5 A. Kerckhoffs and M. J. Langton, *Chem. Sci.*, 2020, **11**, 6325–6331.
- 6 M. Quintana, J. V. Alegre-Requna, E. Marqués-López, R. P. Herrera and G. Triola, *MedChemComm*, 2016, **7**, 550–561.
- 7 S. Zhang, Y. Wang, W. Xie, E. N. W. Howe, N. Busschaert, A. Sauvat, M. Leduc, L. C. Gomes-da-Silva, G. Chen, I. Martins, X. Deng, L. Maiuri, O. Kepp, T. Soussi, P. A. Gale, N. Zamzami and G. Kroemer, *Cell Death Dis.*, 2019, **10**, 242.
- 8 H. Li, H. Valkenier, A. G. Thorne, C. M. Dias, J. A. Cooper, M. Kieffer, N. Busschaert, P. A. Gale, D. N. Sheppard and A. P. Davis, *Chem. Sci.*, 2019, **10**, 9663–9672.
- 9 E. T. Buurman, M. A. Foulk, N. Gao, V. A. Laganas, D. C. McKinney, D. T. Moustakas, J. A. Rose, A. B. Shapiro and P. R. Fleming, *J. Bacteriol.*, 2012, **194**, 5504–5512.
- 10 D. Quiñonero, R. Prohens, C. Garau, A. Frontera, P. Ballester, A. Costa and P. M. Deyà, *Chem. Phys. Lett.*, 2002, **351**, 115–120.
- 11 S. Cohen and S. G. Cohen, *J. Am. Chem. Soc.*, 1966, **88**, 1533–1536.
- 12 A. P. Davis, S. M. Draper, G. Dunne and P. Ashton, *Chem. Commun.*, 1999, 2265–2266, DOI: [10.1039/A907179B](https://doi.org/10.1039/A907179B).
- 13 G. Picci, I. Carreira-Barral, D. Alonso-Carrillo, D. Sanz-González, P. Fernández-López, M. García-Valverde, C. Caltagirone and R. Quesada, *Supramol. Chem.*, 2020, **32**, 112–118.
- 14 S. Camiolo, P. A. Gale, M. B. Hursthouse, M. E. Light and A. J. Shi, *Chem. Commun.*, 2002, 758–759, DOI: [10.1039/B200980C](https://doi.org/10.1039/B200980C).
- 15 C. Caltagirone, G. W. Bates, P. A. Gale and M. E. Light, *Chem. Commun.*, 2008, 61–63, DOI: [10.1039/B713431B](https://doi.org/10.1039/B713431B).
- 16 L. Qin, A. Hartley, P. Turner, R. B. P. Elmes and K. A. Jolliffe, *Chem. Sci.*, 2016, **7**, 4563–4572.
- 17 L. Qin, S. J. N. Vervuurt, R. B. P. Elmes, S. N. Berry, N. Proschogo and K. A. Jolliffe, *Chem. Sci.*, 2020, **11**, 201–207.
- 18 H. Liu, C. S. Tomooka and H. W. Moore, *Synth. Commun.*, 1997, **27**, 2177–2180.
- 19 F. P. Schmidtchen, *Angew. Chem., Int. Ed. Engl.*, 1977, **16**, 720–721.
- 20 N. Busschaert, R. B. P. Elmes, D. D. Czech, X. Wu, I. L. Kirby, E. M. Peck, K. D. Hendzel, S. K. Shaw, B. Chan, B. D. Smith, K. A. Jolliffe and P. A. Gale, *Chem. Sci.*, 2014, **5**, 3617–3626.
- 21 P. Pracht, F. Bohle and S. Grimme, *Phys. Chem. Chem. Phys.*, 2020, **22**, 7169–7192.
- 22 C. P. Kelly, C. J. Cramer and D. G. Truhlar, *J. Phys. Chem. B*, 2007, **111**, 408–422.



23 X. Ni, X. Li, Z. Wang and J.-P. Cheng, *Org. Lett.*, 2014, **16**, 1786–1789.

24 C. Hansch, A. Leo and R. W. Taft, *Chem. Rev.*, 1991, **91**, 165–195.

25 R. B. P. Elmes, P. Turner and K. A. Jolliffe, *Org. Lett.*, 2013, **15**, 5638–5641.

26 M. Ximenis, E. Bustelo, A. G. Algarra, M. Vega, C. Rotger, M. G. Basallote and A. Costa, *J. Org. Chem.*, 2017, **82**, 2160–2170.

27 D. Brynn Hibbert and P. Thordarson, *Chem. Commun.*, 2016, **52**, 12792–12805.

28 <https://supramolecular.org>.

29 N. Busschaert, I. L. Kirby, S. Young, S. J. Coles, P. N. Horton, M. E. Light and P. A. Gale, *Angew. Chem., Int. Ed.*, 2012, **51**, 4426–4430.

30 K. J. Winstanley and D. K. Smith, *J. Org. Chem.*, 2007, **72**, 2803–2815.

31 P. V. Santacroce, J. T. Davis, M. E. Light, P. A. Gale, J. C. Iglesias-Sánchez, P. Prados and R. Quesada, *J. Am. Chem. Soc.*, 2007, **129**, 1886–1887.

32 J. D. E. Lane, S. N. Berry, W. Lewis, J. Ho and K. A. Jolliffe, *J. Org. Chem.*, 2021, **86**, 4957–4964.

33 L. A. Jowett and P. A. Gale, *Supramol. Chem.*, 2019, **31**, 297–312.

34 R. B. P. Elmes, N. Busschaert, D. D. Czech, P. A. Gale and K. A. Jolliffe, *Chem. Commun.*, 2015, **51**, 10107–10110.

35 E. N. W. Howe, N. Busschaert, X. Wu, S. N. Berry, J. Ho, M. E. Light, D. D. Czech, H. A. Klein, J. A. Kitchen and P. A. Gale, *J. Am. Chem. Soc.*, 2016, **138**, 8301–8308.

36 N. Busschaert, S. J. Bradberry, M. Wenzel, C. J. E. Haynes, J. R. Hiscock, I. L. Kirby, L. E. Karagiannidis, S. J. Moore, N. J. Wells, J. Herniman, G. J. Langley, P. N. Horton, M. E. Light, I. Marques, P. J. Costa, V. Félix, J. G. Freya and P. A. Gale, *Chem. Sci.*, 2013, **4**, 3036–3045.

